Thermal performance with depth: Comparison of a mesophotic scleractinian and an antipatharian species subjected to internal waves in Mo'orea, French Polynesia

Mathilde Godefroid, Philippe Dubois, Under The Pole Consortium, Laetitia Hédouin

Thermal performance with depth: comparison of a mesophotic scleractinian and an antipatharian species subjected to internal waves in Mo'orea, French Polynesia

Mathilde Godefroid[1], Philippe Dubois[1], Under The Pole Consortium[2], Laetitia Hédouin[3,4]

[1]Laboratoire de biologie marine, Université Libre de Bruxelles, Avenue F.D. Roosevelt 50, CP160/15, 1050 Bruxelles, Belgium

[2]Under The Pole, 29900 Concarneau, France

[3]PSL Research University: EPHE-CNRS-UPVD, USR 3278 CRIOBE, BP 1013, 98729 Papetoai, Mo'orea, French Polynesia

[4]Laboratoire d'Excellence « CORAIL», Mo'orea, French Polynesia

Corresponding author

Mathilde Godefroid, mathilde.an.godefroid@ulb.be

Université Libre de Bruxelles, Avenue F.D. Roosevelt, 50, CP160/15, 1050 Bruxelles

Abstract

Local thermal environment has a strong influence on the physiology of marine ectotherms. This is particularly relevant for tropical organisms living close to their thermal optimum, well exemplified by the increasing frequency of bleaching occurrence in shallow-water corals. Mesophotic Coral Ecosystems (MCEs) were suggested as potential oases, especially when they are submitted to internal waves inducing short-term cooling events. Indeed, probability of bleaching occurrence in scleractinians was reported to decrease with depth in Mo'orea as temperature variability increases. However, ecophysiological data are currently lacking to understand the cause of lower susceptibility/increased plasticity of deeper corals. A growing interest has been devoted the last decade to MCEs, but our understanding of the physiological performance of benthic organisms living in this environment remains relatively unexplored. To tackle that question, we first compared the metabolic responses (dark respiration, net photosynthesis and photosynthetic efficiency) of the depth-generalist scleractinian *Pachyseris speciosa* from two heterogeneous thermal environment (25 and 85m depths) to acute heat stress to determine if the local thermal environment could predict coral response to warming. Then, we tested the thermal performance of two sympatric species (the scleractinian *P. speciosa* and the antipatharian *Stichopathes* sp.) to determine if there are inter-species differences in performances in species experiencing identical levels of temperature variability, at mesophotic depths (85m). Results revealed broader thermal performances in the mesophotic *P. speciosa* compared to mid-depth ones, and constrained performances in the mesophotic antipatharian compared to the scleractinian species. We hypothesize that the high fluctuations in temperature due to internal waves in deeper areas contribute to the broader thermal performances of mesophotic *P. speciosa.* However, the constrained performances of the mesophotic antipatharian compared to *P. speciosa* suggests that other processes than the symbiosis with zooxanthellae also influence thermal performances of these mesophotic organisms. Our results supported that *Stichopathes* sp. lives close to its thermal optimum, suggesting a (relatively) cold thermal specialist strategy. In this context, composition of MCEs in the

future is unlikely to shift to antipatharian-dominated landscape and will remain coral-dominated landscape.

Keywords

Global warming, Thermal acclimatization, Mesophotic, Scleractinian, Antipatharian, Performance curve, Environmental variability

Introduction

Janzen (1967) hypothesized that the physiological tolerance of each organism should be large enough to encompass the entire gradient of conditions experienced throughout its life. This hypothesis influenced theoretical models in suggesting that organisms from more variable climate should be under selection for greater thermal acclimation ability than those from more stable climate ("The climate variability hypothesis"; Angilletta, 2009; Ghalambor, 2006; Gunderson & Stillman, 2015; Tewksbury et al., 2008). Evidence in favour with this hypothesis has been accumulating, with studies indicating that tropical organisms have narrower thermal window of performance (Thermal breadth, T_{br}) than temperate species, because their seasonal thermal range is smaller (Deutsch et al., 2008; Gaston et al., 2009; Ghalambor, 2006; Huey et al., 2009; Sunday et al., 2012; Tewksbury et al., 2008). However, contrasting evidence were also obtained and suggested to reflect the influence of local/regional thermal variation in shaping thermal acclimation (Angilletta, 2009; Seebacher et al., 2015; Shah et al., 2017a, 2017b). For example, experimental studies in the marine environment showed differences in heat stress tolerance across reef sites characterized by contrasting levels of thermal variability (i.e. fore-reef *vs* back-reef, inshore *vs* offshore reef ; Barshis et al., 2018; Kenkel et al., 2013, 2015; Oliver & Palumbi, 2011).

Depth may also influence thermal variability, with shallow depths experiencing larger variations than subjacent mesophotic depths, which have long been considered as cooler and more stable thermally (Bongaerts et al., 2010; Glynn, 1996; Turner et al., 2019). Therefore, organisms from mesophotic depths were hypothesized to have higher thermal sensitivities than shallow water ones (Smith et al., 2016). This has been supported by some studies (Frates et al., 2021; Smith et al., 2016) but contrasting evidence arose from physiological measurements and bleaching events (Frade et al., 2018; Gould et al., 2021; Rocha et al., 2018). Now, thermal stability of mesophotic environments may be compromised by cold water intrusions due to oscillations of water column isotherms, mixing, internal waves and tides (Leichter et al., 2006, 2012, 2014; Sheppard, 2009; Wall et al., 2015; Wolanski et al., 2004; Wyatt et al., 2020). Internal waves are created by the rise of cold and nutrient-rich waters being uplifted up the reef slope, inducing thermal fluctuations at the time scale of hours to days which often exceed the magnitude of temperature fluctuations in shallow waters (Godefroid et al., 2022; Leichter et al., 2012). This cold water flushes to mesophotic depths may alleviate cumulated thermal stress during heat waves, resulting, for instance, in reduced scleractinian bleaching (Pérez-Rosalez et al., 2021; Storlazzy et al., 2020; Wall et al., 2015; Wyatt et al., 2020) but, to our knowledge, it has never been addressed if such transient cold thermal variability resulted in increased thermal tolerance (wider T_{br}) of mesophotic organisms.

Mesophotic Coral Ecosystems (MCEs) are characterized by the presence of light-dependent corals and associated communities, typically from around 30m depth and extending up to 150m in certain regions (Hinderstein et al., 2010; Lesser et al., 2009). In tropical zones, scleractinian corals usually dominate in shallow waters (when conditions are appropriate), with some species extending their range to mesophotic depths. Reef community composition progressively shifts with depth and non-photosynthetic organisms become dominant when light conditions do not meet the requirements for scleractinian photosynthesis (Pyle et al., 2019).

Among these, antipatharians are particularly abundant at mesophotic depths, sometimes forming dense aggregations called Marine Animal Forests (MAFs, *sensu* Rossi et al., 2017), and even becoming

dominant at depth in several regions. Their role as habitat providers and nursery areas then become fundamental to the maintenance of ecosystem functions (Bo et al., 2014, 2019; De Clippele et al., 2019; Terrana et al., 2019). They differ from scleractinians because they are commonly referred to as azooxanthellate, with only a few specimens showing the presence of Symbiodiniaceae/Symbiodiniaceae-like cells (Bo et al., 2011; Gress et al., 2021; Wagner et al., 2011). They also differ from scleractinians by their proteinaceous (and not calcareous) skeleton (Opresko et al., 2014; Wagner et al., 2012).

To date, one study only has addressed the thermal sensitivity of a single antipatharian species and revealed that it lives close to its T_{opt} (at least during the coldest months of the year) and has a rather narrow T_{br} (tropical mesophotic *Stichopathes* sp., 15 days of exposure; Godefroid et al., 2022). This experiment was conducted in the island of Mo'orea in French Polynesia, which is known to be characterized by strong internal wave activity that impacts reef slopes at depths ≥30m around the entire island (Leichter et al., 2012). Superimposed on seasonal temperature changes of approximately 3°C, internal waves create a pattern of high frequency temperature variation that is created by the arrival of cold and nutrient rich waters (Leichter et al., 2012). The amplitude of these fluctuations increases with depth and are modulated across seasons, with markedly higher internal waves activity from Oct-May than from Jun-Sep (Godefroid et al. 2022, Leichter et al. 2012, Pichon, 2019, Wyatt et al. 2020). Over a 40-days period during the cold season (Oct-Nov 2019), which coincides with the period of high internal wave activity, mean daily temperature fluctuations were twice as large at 90m than at 20m and the total temperature range over this period was 4.6°C at 90m *vs* 2.9°C at 20m (Godefroid et al. 2022). This indicates that mesophotic depths in Mo'orea are more variable than shallow-water ones, at least during the cold season (Godefroid et al., 2022).

The aim of the present study was first to assess how the thermal physiology of a generalist coral living from mid-depth (25m) to mesophotic (85m) environment, characterised by distinct temperature regimes (warmer and less variable in shallower part of the reefs), varies along the depth gradient in Mo'orea. We established TPCs for respiration, photosynthetic efficiency (F_v/F_m) and net photosynthesis (P_{net}) of these two populations of *Pachyseris speciosa* living in different environments, using a short-term ramping method. We hypothesized that TPCs should differ across the depth gradient, with lower T_{opt} and wider T_{br} for mesophotic *P. speciosa* than for mid-depth ones. Secondly, we investigated the thermal performance of two sympatric species (the scleractinian *Pachyseris speciosa* and the antipatharian *Stichopathes sp.*) exposed to identical thermal regime (mesophotic zone, 85m). We established TPCs for respiration (both species), photosynthetic efficiency (F_v/F_m) and net photosynthesis (*P. speciosa*), their shapes and positions, to investigate the inter-specific variation of thermal strategy in mesophotic environment. Understanding thermal performance strategy and plasticity of key benthic organisms living in mesophotic areas will be an asset to better predict how climate change will shape the future of the reefs from shallow to mesophotic areas.

Materials and Methods

Coral collection and acclimation

Coral colonies were collected on the outer reef slope on the North shore of the island of Mo'orea (17°28'41.7''S, 149°51'09.9''W). The fore reefs on the North coast of Mo'orea are characterized by a gentle slope (40-60°) from the surface down to 70-80m depth, where it drops almost vertically (inclination of 60% or more) (Pérez-Rosales et al., 2021). Between 30 and 70m depth, the substrate is mainly covered by sedimentary deposits, known as the "sandy plain", which is virtually devoid of sessile benthos, except in some parts where there is an almost continuous monospecific cover of the substratum (up to 70-80%) by *Pachyseris speciosa*, over large areas (Pichon, 2019). *P. speciosa* is a

keystone mesophotic species that is very common and widespread in the Society and Tuamotu Archipelagos (Pichon, 2019).

On February 11th, 2021, the team of technical divers from *Under The Pole* expeditions (https://www.underthepole.com/) collected eight colonies of the antipatharian *Stichopathes* sp. and eight colonies of the scleractinian *P. speciosa* on a vertical slope at 85m depth. For the taxonomic determination of *Stichopathes* sp., preliminary analyses targeted the nuclear Internal Transcribed Spacers of the ribosomal DNA (ITS1) and suggested this *Stichopathes* sp. to be part of clade C as described in Bo et al. (2012). All colonies were immediately transported to the "Centre de Recherches Insulaires et Observatoire de l'Environnement" (CRIOBE), fragmented on the same day (two fragments per colony for *Stichopathes* sp. and four fragments per colony for *P. speciosa*) and placed in an open-circuit and sand-filtered aquarium with parameters of the collection site (Volume: 200L, Temperature: 26°C, salinity: 35.5). Light was controlled using AquaIllumination Hydra lamps (USA) in the blue spectrum (4-15 µmol photons m^{-2} s^{-1}). The same day, eight colonies of *P. speciosa* were also collected at 25m depth (gentle slope inclination), on the same site than the mesophotic colonies (17°28'41.7''S, 149°51'09.9''W). They were transported to the CRIOBE and immediately fragmented (four fragments per colony) and placed in another sand-filtered aquarium with parameters of the corresponding site (Volume: 200L, Temperature: 28°C, salinity: 35.5, light: 200-250 µmol photons m^{-2} s^{-1} in the baseline spectrum). These depths (25 and 85m) were selected as 25m corresponds to the upper bathymetric range of *P. speciosa* in Mo'orea, extending at least up to 85m, corresponding to the upper bathymetric range of *Stichopathes* sp., while remaining accessible to technical divers. A complete characterization of the thermal environment of this site at different depths was reported in Godefroid et al. (2022) The surface area of the *P. speciosa* fragments was measured using a high-quality 3D scanner (EinScan-SP Scanner, Shining 3D, China). The black and reflective properties of the skeleton prevented the use of the scanner for *Stichopathes* sp., so its surface area was calculated based on the surface formula of a cylinder. Surface areas of the fragments were 5.1 ± 0.3 cm^2 (n=21) for *Stichopathes* sp., 79.9 ± 3.9 cm^2 (n=24) and 71.2 ± 2.3 cm^2 (n=26; mean ± se) for *Pachyseris speciosa* 25 and 85m, respectively.

164 The fragments were left five days to recover and then temperature in both aquaria was gradually
165 decreased/increased by 0.5°C/day to reach a final common temperature at 27°C (i.e. the acclimation
166 temperature). 27°C was selected as it is the average temperature between both depths at the time of
167 collection and it is within the annual range of temperature for both depths. When the target
168 temperature of 27°C was reached, the fragments were left to acclimate to these new conditions for at
169 least ten days before starting the ramp experiments. The experiment time schedule is depicted in
170 Figure 1a.

171

172 *Aquarium conditions*

173 Once at the target acclimation temperature (27°C), the only parameter that differed between the
174 aquaria was light, and all other parameters were manipulated identically. Both aquaria were open-
175 circuit, with seawater pumped at 25m depth in the Bay in front of the facilities and sand and UV
176 filtered. Temperature was manipulated using water chillers (one per aquarium, TECO TK1000, Italy)
177 and light was provided using AquaIllumination Hydra (one per aquaria, USA) following the natural diel
178 cycle. From 05:30 to 10:00 am, light was ramped up to a maximum (around 200-250 µmol photons m^{-2}
179 s^{-1}, using the baseline spectrum provided by the AquaIllumination Hydra lamps, for 25m and 4-15
180 µmol photons m^{-2} s^{-1}, in the blue spectrum, for 85m), which was maintained until 2 pm, before ramping
181 down to total darkness at 6 pm. Light intensity was selected based on *in situ* data from 20 and 90m
182 collected using light loggers (DEFI2-L, JFE Advantech Co., Japan). As *Stichopathes* sp. depends on
183 heterotrophic feeding, both aquaria were fed daily with a mix composed of live *Artemia salina*,
184 copepods and phytoplankton.

185 The respirometry experiments were run in a separate system composed of an open-circuit buffer tank
186 (150 L) where the temperature was manipulated, connected with a pump system to an experimental
187 tank (55 L) where the respirometry chambers were installed for the respirometry analyses. The
188 experimental tank was overflowing into the buffer tank and excess seawater in the buffer tank was

189 removed from the system by overflow. The buffer tank and the experimental tank were equipped with
190 circulation pumps to ensure a complete homogenisation of the temperature in both tanks. The high
191 volume of seawater (200 L) in the system and the fact that temperature was only manipulated in the
192 buffer tank allowed maintaining a very stable temperature in the experimental tank at all stages of the
193 experiments. Moreover, the open-circuit system ensured that the accumulation of catabolism and
194 stress molecules or mucus produced by the fragments during respirometry measurements would be
195 eliminated between each measurement period, thus allowing good water quality throughout the
196 experiments. Temperature in the buffer tank was controlled using one chiller (TECO TK2000, Italy) and
197 three titanium heaters (Schego, Germany), each connected to a temperature controller (ITC-308,
198 Inkbird, China). This allowed increasing water temperature quickly between the experimental stages.
199 A bubbling system was installed in the experimental tank to increase seawater aeration.

200

201 *Thermal ramping assays*

202 Ramp experiments were performed to determine the TPCs of respiration (R_{dark}; *Stichopathes* sp. and
203 *P. speciosa*), photosynthesis (P_{net}) and photochemical efficiency (F_v/F_m) (*P. speciosa* only as
204 *Stichopathes* sp. does not host zooxanthellae). Each ramp experiment was divided in two legs, both
205 starting at the acclimation temperature: a hot ramp (27, 28, 29, 30, 31, 32°C) and a cold ramp (27, 26,
206 25, 24, 23°C). Four experiments were performed in the dark to assess the TPCs for R_{dark} and F_v/F_m. One
207 fragment from eight *Pachyseris speciosa* 25m colonies, eight *Pachyseris speciosa* 85m colonies and
208 eight *Stichopathes* sp. colonies was used for the hot ramp and another (from the same colony) for the
209 cold ramp. This way, a fragment was only used in a single hot ramp experiment (and was not reused)
210 and another fragment from the same colony for the cold ramp. In total, eight independent replicates
211 (colonies) per species/population were tested for each leg of the ramp experiment, with paired (from
212 the same colony) replicates between cold and hot ramps.

213 Ramp experiments were performed similarly under light to assess the TPCs for P_{net}. As light intensity
214 decreases with depth, distinct ramps were performed for *P. speciosa* 25m and 85m, at the respective
215 light intensities used for the acclimation period. One hot and one cold ramp were performed on
216 fragments from 5 colonies for *P. speciosa* 25m and the same on fragments from 5 colonies for *P.*
217 *speciosa* 85m. So, a total of 5 independent replicates (colonies) per population were tested for each
218 leg of the ramp experiment, with paired (from the same colony) replicates between cold and hot
219 ramps.

220 Each ramp experiment proceeded similarly, with six cycles of a hot ramp (on day 1), followed by a cold
221 ramp (on day 2) performed on another fragment from the same colonies. For example, in the case of
222 the hot ramp experiments in the dark, six coral fragments were moved from their aquarium at about
223 6 am to one of the eight respirometry chambers that were held in the experimental tank at 27°C (Fig.
224 1b). After 1 hour of acclimation in either dark or light conditions (i.e. light intensity corresponded to
225 the maximum light intensity used in the acclimation tank), the chambers were closed and oxygen
226 consumption was measured for 40 min to estimate R_{dark} or P_{net}. Then, the chambers were opened in
227 the experimental tank (allowing water exchange between the water in the chambers and from the
228 experimental tank) and F_v/F_m was measured in triplicate for each fragment (only in the dark
229 incubations) before increasing the temperature to the next target temperature (+1°C), for one hour
230 (i.e. 30-min temperature increase and 30-min of acclimation to the new temperature). Then, the
231 chambers were sealed again to start a new 40-min measurement period to estimate R_{dark} or P_{net}. The
232 same procedure was repeated until the full range of experimental temperatures had been tested (up
233 to 32°C), after which temperature was decreased back to 27°C in one step (i.e. the acclimation
234 temperature) and new measurements of oxygen consumption were taken after 2.5 (around 7 pm) and
235 12 hours (the next morning) to evaluate the recovery capacity of the fragments (Fig. 1b). Between the
236 end of the ramp experiment and the 2.5 and 12h "recovery" measurements, chambers were opened
237 and water exchanged with the water of the experimental tank. For the cold ramp experiments, the

same procedure (acclimation, measurement of R_{dark} or P_{net}, then F_v/F_m) was followed at 27, 26, 25, 24 and 23°C but the recovery capacity was not assessed at the end.

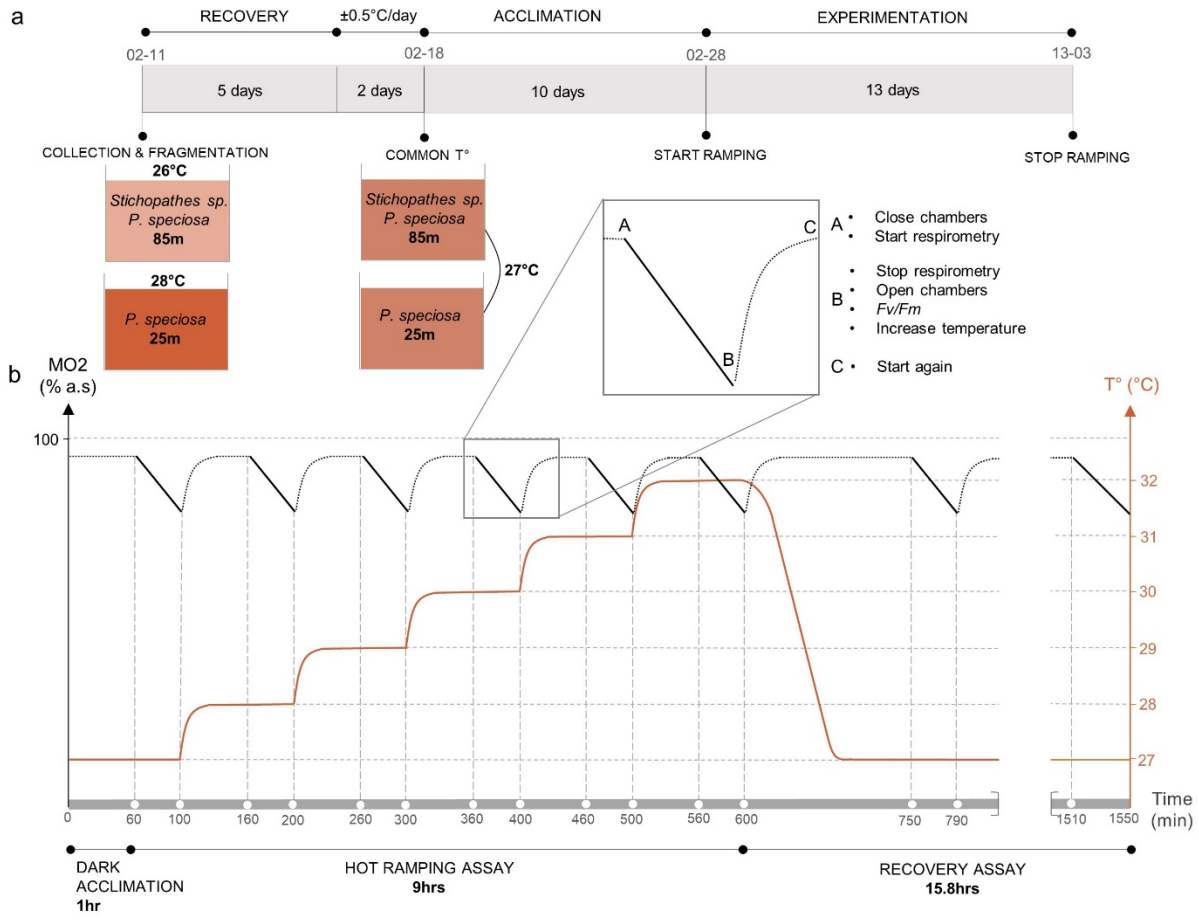

Figure 1. (a) Time schedule of the experiments with coral collection and fragmentation, post-fragmentation recovery (5 days), temperature increase/decrease to reach the common temperature at 27°C (2 days), acclimation at 27°C (10 days) and experimentation (hot and cold ramps, 13 days). (b) Schematic representation of a hot ramp with (1) 1 hour dark acclimation, (2) 9 hours of hot ramping assays (respirometry and photosynthetic efficiency (F_v/F_m) measurements, at 27, 28, 29, 30, 31 and 32°C) and (3) 15.8 hours of recovery assay (the water temperature is brought back to 27°C and measurements of oxygen consumption rates are taken 2.5 and 12 hours after the last test at 32°C).

Metabolic responses

Metabolic rates (R_{dark} and P_{net}) were determined by measuring changes in dissolved oxygen concentration in eight respirometry chambers simultaneously. Measurements were taken every 5 s using fiber-optic oxygen sensors connected to two 4-channel Fiber Optic Oxygen Transmitter (OXY-4 SMA G2 and OXY-4 SMA G3, Pre-Sens Precision Sensing GmbH, Germany), and were measured as saturation level (%) using the software PreSens Measurement Studio. The eight respirometry chambers varied in volume according to the species: fragments of *Stichopathes* sp. (unbranched, long and thin corallum) were placed in Falcon tube of ~50 mL and fragments of *P. speciosa* (flat and thin) were placed in plastic chambers of ~200 mL. In each chamber, an oxygen sensor spot (PreSens SP-PSt3-NAU-D5-YOP-SA) was glued and calibrated according to the supplier's manual and a magnetic stir bar was used (and separated from the fragment by a mesh) to maintain constant homogenization of the water in the chamber. The chambers were submerged in a recirculating water bath (as previously mentioned) which was placed on top of eight individual magnetic stirring plates allowing the constant functioning of the magnetic stir bars in the chambers. Oxygen saturation was recorded in a blank chamber (free of coral fragment) during each measurement and two blank chambers were used when the two types of chambers (50 mL and 200 mL) were used during the same experiment (dark ramps). These blanks allowed measuring the background respiration (i.e. the part of the respiration attributed to the seawater microbes). At the end of the measurements, the surface area of the fragments was measured as previously described. Oxygen saturation measurements were normalized based on the volume of seawater in the experimental chambers (V), calculated from the density of seawater (Millero & Huang, 2009; Millero & Poisson, 1981). Oxygen saturation was then converted to oxygen concentration and the rate of oxygen consumption (VO_2) was calculated from the slope of its linear regression $\left([O_2]_{t_0} - [O_2]_{t_1}\right)$ with time (t):

$$VO_2 = \left\{\left[\left([O_2]_{t_0} - [O_2]_{t_1}\right) * \frac{V}{t}\right] - \left[\left(\left[O_{2,blank}\right]_{t_0} - \left[O_{2,blank}\right]_{t_1}\right) * \frac{V_{blank}}{t}\right]\right\} * \frac{1}{SA}$$

Oxygen consumption rate of the fragments was corrected according to the consumption rate of the seawater-only chamber and normalized using the surface area (SA) of the fragments, and was expressed in micromole of oxygen per square centimetre per hour.

At the end of each metabolic rate measurements, all respirometry chambers were opened in the experimental tank and the performance of the *Symbiodiniacea* hosted by fragments of *P. speciosa* was quantified by measuring their photochemical efficiency (F_v/F_m), in triplicate per fragment. These measurements were repeated at each temperature of all ramp experiments performed in the dark using a pulse-amplitude modulation fluorimeter (Diving-PAM, Walz, Germany). Dark-acclimated F_v/F_m should decrease if the symbionts become thermally stressed (Aichelman et al., 2019; Fitt et al., 2001; Thornhill et al., 2008; Warner et al., 1996). P_{gross}, the total amount of oxygen produced by the fragments, was calculated by adding R_{dark} to P_{net}.

Statistical analyses

All data were analysed using the statistical software R version 1.3.959 (R Core Team, 2020).

Non-linear least-square regression models were fitted to the variables R_{dark} for *Stichopathes* sp. and F_v/F_m for *P.speciosa*, using a symmetrical Gaussian function (as recommended by Angilletta, 2006, and widely used since, see *e.g.* Rodolfo-Metalpa et al., 2014, Jurriaans et al., 2019, 2020) with the R package *nlstools* (Baty et al., 2015):

$$P = Pf_{max} * \exp\left(-0.5\left(\frac{T-T_{opt}}{T_{br}}\right)^2\right) \quad (1)$$

where P is the physiological response, Pf_{max} is the maximum value of that response, T_{opt} is the temperature at which the response value is maximal (i.e. the mean of the Gaussian function) and T_{br} is the breadth of the response curve (i.e. the standard deviation of the Gaussian function). Significant differences between the parameters Pf_{max}, T_{opt} and T_{br} were defined as non-overlapping 95% confidence intervals.

298 Simple linear regression models ($y = ax + b$) were fitted to the variables R_{dark}, P_{net} and P_{gross} for *P.*
299 *speciosa*, with temperature as independent variable (n=10). Comparison of slopes were performed
300 using the R package *lsmeans* (Russel, 2016).

301 As R_{dark} data were not modelled identically for *Stichopathes* sp. (Gaussian curve) and *P. speciosa* (Linear
302 regression), thermal sensitivity was compared by calculating the temperature coefficient Q_{10} (i.e. the
303 proportional change of respiration in response to a temperature increase of 10°C) using the van't Hoff
304 equation:

305 $$Q_{10} = \left(\frac{R_2}{R_1}\right)^{\left[\frac{10}{T_2 - T_1}\right]}$$

306 where R_1 and R_2 are the rates of oxygen consumption corresponding to low temperature (T_1) and high
307 temperature (T_2), respectively. Q_{10} was calculated in the range 23-32°C for *P. speciosa* and 23-28°C for
308 *Stichopathes* sp. (in the range of linear increase with temperature). Q_{10} values were first calculated for
309 each individual colony between consecutive temperatures and these were then averaged per
310 population. Q_{10} is typically around 2-3 for physiological processes; a lower Q_{10} indicates that respiration
311 rates were less sensitive to increasing temperatures, whereas a higher Q_{10} indicates higher thermal
312 sensitivity.

313 Analysis of residuals was carried out for all regression analysis. No trend in residuals was evidenced.

314 Recovery capacity for each variable and *P. speciosa* population was evaluated using two-factor mixed
315 model ANOVA, with population and time as fixed cross factors and fragment as a random repeated
316 subject (Doncaster & Davey, 2007). When the interaction was significant, a post-hoc Tukey's test was
317 performed using the appropriate mean square error. R_{dark} for *Stichopathes* sp. was analysed separately
318 using one-factor ANOVA with Time as fixed factor, as the surface values of the two studied species
319 were highly different due to their distinct morphologies (voluminous and flat *vs.* thin and filiform),
320 which strongly influenced the R_{dark} value after normalisation.

321

Results

Metabolic responses with temperature

Dark respiration (R_{dark}) increased linearly with temperature for *P. speciosa* living at 25m (mid-depth colonies) and 85m (mesophotic colonies) (Figure 2a, b; Linear regression, *p<0.001* for both species, Table S1). However, the rate of increase (i.e. the slope of the regression) is significantly higher for the mid-depth than for the mesophotic colonies (Comparison of slopes, *p<0.05*, Table S2). For *Stichopathes* sp., R_{dark} data can be fitted by a nonlinear Gaussian relationship with temperature (Figure 2c). T_{opt} was calculated at 29.6°C, corresponding to a maximum R_{dark} of 0.2 µmol O_2 cm^{-2} h^{-1} (Table S3). Q_{10} was calculated in the linear part of the regression (before T_{opt} for *Stichopathes* sp.) to allow comparing the three groups (*P. speciosa* 25m, 85m and *Stichopathes* sp.). Q_{10} did not differ between depths and stayed around 2-3 for *P. speciosa* , but was much higher and variable for *Stichopathes* sp. (45.68 ± 61.96, mean ± sd n=6) (Table 1).

Absolute values of Net Photosynthesis (P_{net}) were positive at all temperatures for *P. speciosa* 25m but were negative for the mesophotic fragments of *P. speciosa* (Figure 2d, e). At both depth, P_{net} decreased linearly with temperature (Linear regression, *p<0.001* for *P. speciosa* 25m and *p<0.005* for *P. speciosa* 85m; Table S1) but the decrease was significantly more important for the mid-depth fragments (Comparison of slopes, *p<0.05*; Table S2).

The compensatory effect of P_{net} on R_{dark} was assessed by calculating gross photosynthesis. P_{gross} tended to decrease linearly with temperature for mid-depth fragments and increased significantly for mesophotic ones (Linear regression, *p>0.05* for *P. speciosa* 25m and *p<0.001* for *P. speciosa* 85m; Table S1). Comparison of slopes revealed that depth had significant influence on P_{gross} (*p<0.001*), but temperature did not (*p>0.05*; Table S2).

Photosynthetic efficiency (F_v/F_m) can be fitted by a nonlinear Gaussian relationship with temperature, for fragments of *P. speciosa* from both depths (Figure 2f, g). The T_{opt} was 26.2°C for the mid-depth fragments and 27.8°C for the mesophotic ones (corresponding to maximum yields of 0.68 for both

depths). However, confidence intervals overlapped for all the estimated parameters (T_{opt}, T_{br}, $F_v/F_{m\,max}$) for *P. speciosa* 25 and 85m, indicating no significant differences between the two populations for these parameters (Table S3).

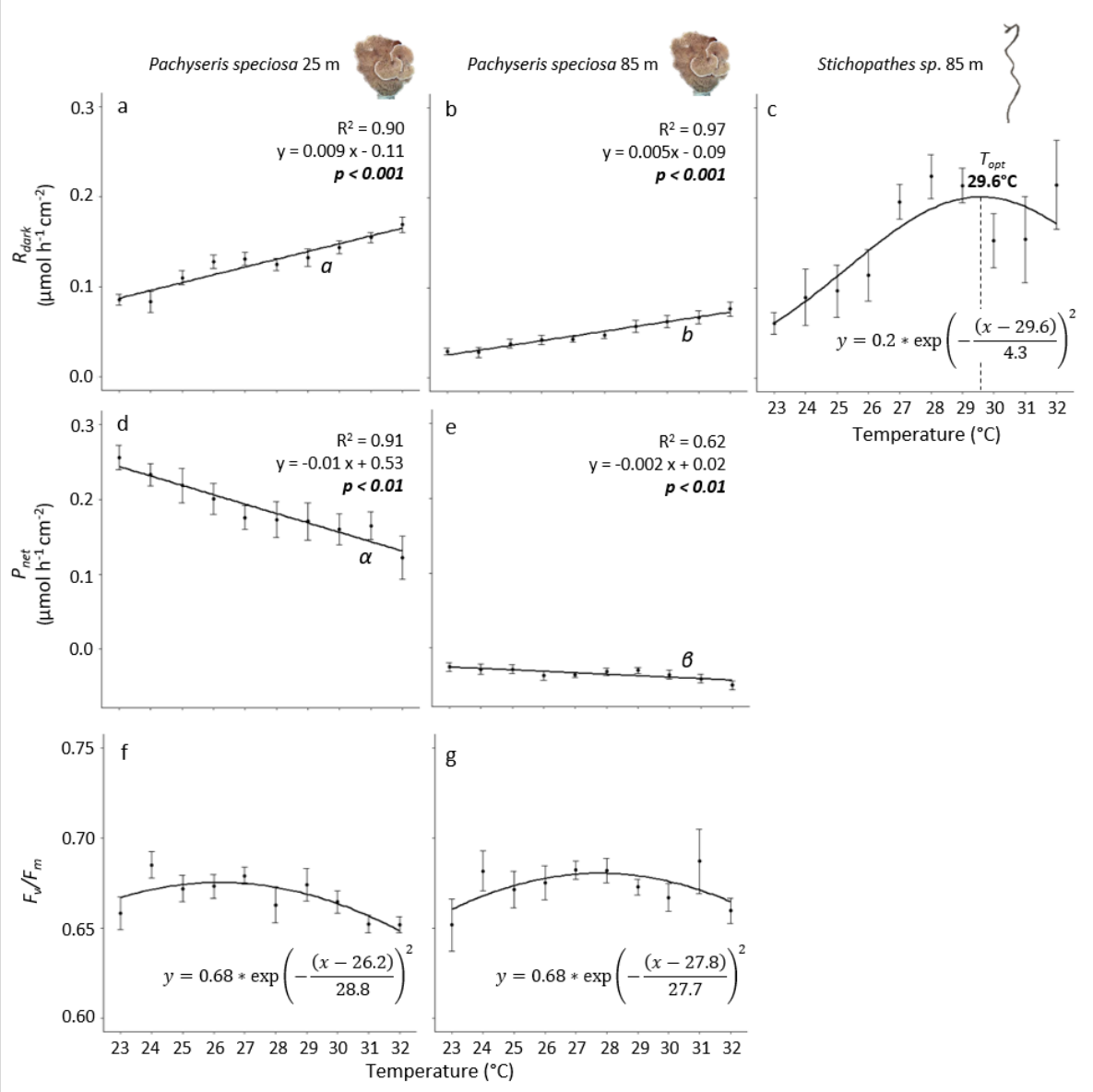

Figure 2. Thermal performance curves for (a-c) Dark Respiration (R_{dark}); (d, e) Net Photosynthesis (P_{net}); (f, g) Photosynthetic efficiency (F_v/F_m) for (a, d, f) *P. speciosa* 25m, (b, e, g) *P. speciosa* 85m and (c) *Stichopathes* sp. Datapoints are the mean values ± se (n=5-8). Data were modelled using simple linear

355 regression (y = ax + b) or nonlinear regression, Gaussian curve, using equation (1). *p*-values of each of
356 the 3 parameters of the Gaussian regressions (c, f, g) are shown in Table S3.

357

358 **Table 1.** Q_{10} (mean ± sd) value for oxygen consumption rate with temperature, calculated for *P.*
359 *speciosa* 25m, 85m and for *Stichopathes* sp. (n=6-8)

	***P. speciosa* 25m**	***P. speciosa* 85m**	***Stichopathes* sp.**
Q_{10}	2.26 ± 0.42	3.29 ± 1.36	45.68 ± 61.96

360

361 *Recovery capacity after the ramping*

362 Recovery capacity was assessed by comparing measures at acclimation temperature before ramping
363 and 2.5 and 12h after ramping and getting back to the acclimation temperature. R_{dark} of *P.speciosa*
364 significantly differed according to depth (Mixed model ANOVA, $p_{depth}<0.001$), time ($p_{time}<0.001$) and
365 the interaction of these factors ($p_{depth * time}$=0.015) Values of R_{dark} were significantly higher for the mid-
366 depth fragments of *P. speciosa* than for the mesophotic ones, at acclimation temperature (27°C) and
367 all recovery stages (p_{Tukey}<0.001; Figure 3a, b; Table S5). In addition, 2.5 hours after being brought back
368 to acclimation temperature, fragments of *P. speciosa* from all depths had a significantly higher
369 respiration rate than before the ramping (p_{Tukey}=0.048 for *P. speciosa* 25m and p_{Tukey}=0.028 for *P.*
370 *speciosa* 85m), but a respiration rate not significantly different from that before the ramping was
371 reached after 12 hours for both populations (p_{Tukey} ≥0.112). For *Stichopathes* sp., there were no
372 significant differences between R_{dark} pre-ramping and post-ramping recovery measurements
373 (p_{time}=0.075) (Figure 3c, Table S4).

374 Absolute values of P_{net} were significantly higher for the mid-depth colonies of *P. speciosa* than for the
375 mesophotic ones (Mixed model ANOVA, $p_{depth}<0.001$; Table S5). The P_{net} of mesophotic *P. speciosa* is
376 so low (around zero) than no effect can be observed. No significant differences were highlighted

between P_{net} values pre-ramping and post-ramping recovery nor the interaction between time and depth (p_{Time}=0.144, $p_{Time*depth}$=0.462) (Figure 3d, e, Table S5).

Photosynthetic efficiencies (F_v/F_m) of fragments of *P. speciosa* did not differ according to depth (Mixed model ANOVA, p_{depth}= 0.370) but were significantly reduced after 2.5 and 12 hours of recovery post-ramping (p_{Time}*<0.001; p_{Tukey} ≤0.013*); the two latter did not differ (p_{Tukey} >0.083; Figure 3f, g; Table S5).

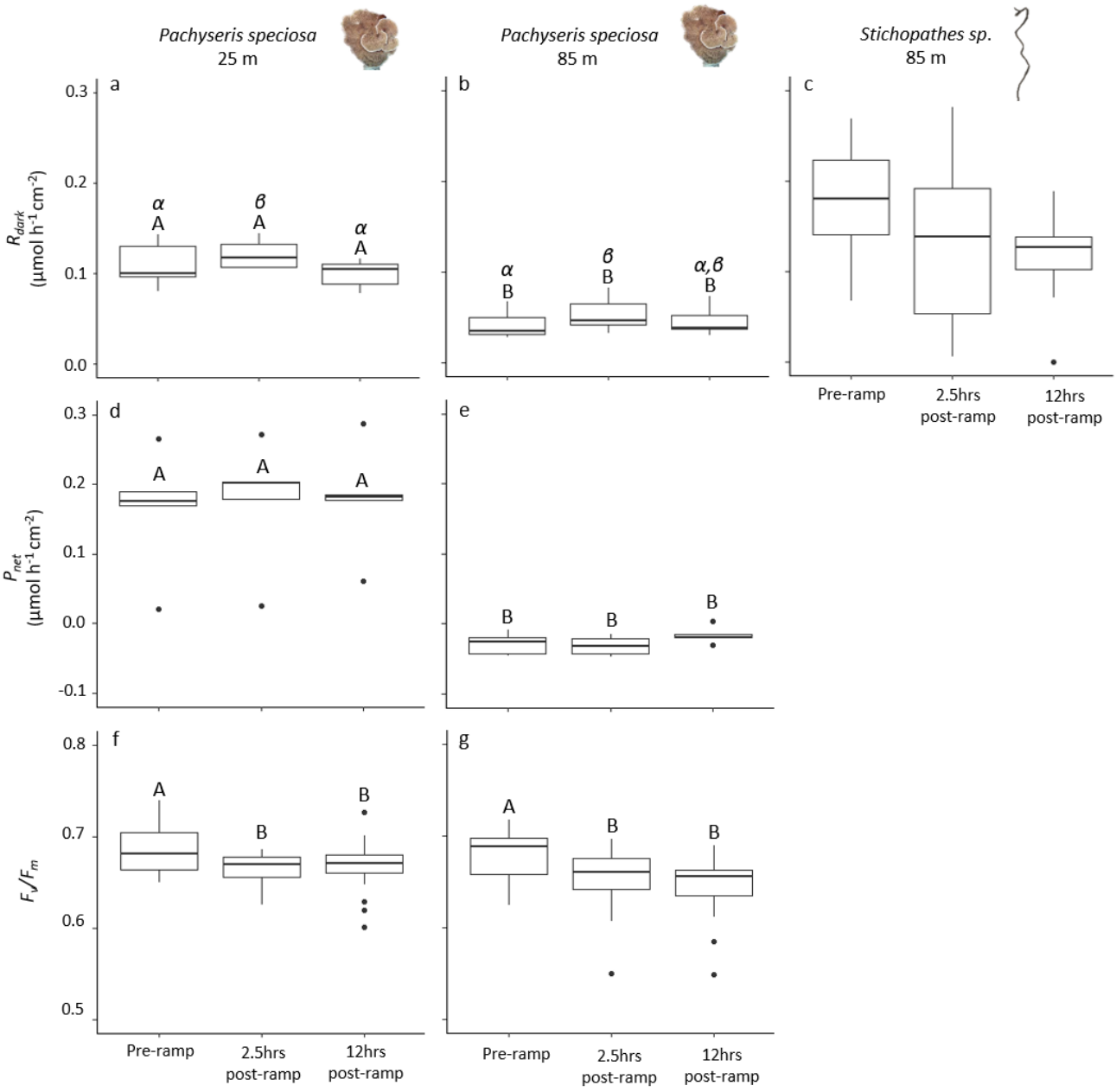

Figure 3. Recovery capacity of (a,d,f) *P. speciosa* 25m, (b,e,g) 85 m and (c) *Stichopathes* sp. Metabolic performances of the coral fragments (n=5-13) before the ramp experiment (27°C, pre-ramp) and after the ramp experiment, when brought back to 27°C for 2.5 and 12 hours (post-ramp). Uppercase letters indicate significant differences between *P. speciosa* 25 and 85m. Greek characters indicates significant differences within a population according to time (Mixed model ANOVA with repeated measures on one cross factor). One-factor ANOVA did not reveal any statistical difference for *Stichopathes* sp. (Tables S4, S5).

Discussion

Ongoing ocean warming is increasingly damaging coral reefs and evidence of mass mortality events are multiplying. Researchers have suggested that depth may provide refuge from events occurring at shallower depth, as heat accumulation decreases with increasing depth (Turner et al., 2019). Yet, evidence from experimental studies, oceanographic thermal models and bleaching events are mixed (Frade et al., 2018; Frates et al., 2021; Gould et al., 2021; Pérez-Rosales et al., 2021; Rocha et al., 2018; Smith et al., 2016; Venegas et al., 2019; Wall et al., 2015). Differences in sensitivity across depths can be attributed to differing environmental conditions and/or species physiological capacities (Page et al., 2019). While abiotic differences across depths have been addressed multiple times, intrinsic metabolic differences have not yet received much attention (Ferrier-Pagès et al., 2022).

Pachyseris speciosa 25m *vs.* 85m

In this study, we assessed the thermal performance of the photosynthetic scleractinian *Pachyseris speciosa* from distinct depths (25 and 85m). Given the cooler mean temperatures and highly fluctuating thermal conditions (owing to internal waves) at mesophotic depths in Mo'orea (Leichter et al., 2012; Godefroid et al., 2022), we expected that mesophotic colonies of *P. speciosa* would have lower T_{opt} and wider T_{br} compared to mid-depth colonies. T_{opt} was not reached by specimens from both depths for respiration and photosynthesis: performances increased linearly with temperature, so we could not determine T_{opt} nor T_{br} for *P. speciosa.* This is likely related to the experimental protocol used: longer exposure time or further temperature increase (above 32°C) could allow achieving T_{opt}. Despite this, the effect on performances (i.e. the slope or the rate of activation, E_a) was higher on mid-depth than on mesophotic colonies, suggesting that mesophotic colonies have a higher capacity to encompass large range of temperatures and will be less affected by temperature regimes higher than T_{opt}, compared to their mid-depth congeners.

Symbiont density, that was not assessed in the present study, might be one of the factors influencing depth-specific thermal performance in terms of respiration. Photoacclimatation is a well-known process in corals, allowing to maintain efficient performance in distinct light intensity regimes. In low light environment as in mesophotic depths, contrasting results were reported, showing in some cases an increase, decrease or stable symbiont density (Fitt et al., 2000; Leletkin et al., 1996; Mass et al., 2010; Padilla-Gamino et al., 2019; Smith et al., 2017). Our data revealed a higher photosynthetic rates (P_{net}) in mid-depth than in mesophotic fragments, which may be due to higher symbiont density and/or chlorophyll pigments. Differences in thermal performance across depths could also be related to the composition in Symbiodiniaceae, but previous research in Mo'orea showed that *Symbiodiniaceae* and bacterial communities did not differ across depths (6-120m) for *P. speciosa* (Rouzé H., unpublished results).

Photoacclimatation is not the main or single driver modulating the capacity of corals to thrive under fluctuating environmental conditions. Other parameters, such as changes in colony morphology or in the contribution of heterotrophy, through feeding, are also known to differ across depths (Kahng et al., 2019). In the present study, we did not characterize the heterotrophic contribution of corals along the depth gradient. So, we cannot exclude that the heterotrophic energy input through feeding, that is known in some cases to represent an important contribution in the mesophotic corals (Kahng et al., 2019), will affect thermal performance. Further research will be required to determine the role of photo-physiological capacities and heterotrophy into the performance of corals from distinct depths.

Another factor that is likely to influence the thermotolerance of *P. speciosa* from different depths is the adaptation and/or acclimatization of the corals to the local temperature regime. A large body of research on scleractinian corals showed that thermal history, in particular temperature variability, affects coral physiological tolerance under heat stress (Barshis et al., 2018; Castillo & Helmuth, 2005; Guest et al., 2012; Kenkel et al., 2013, 2015; Oliver & Palumbi, 2011; Safaie et al., 2018). However, research that have experimentally compared thermal sensitivity of coral conspecifics from distinct

depths are relatively scarce. These studies either found no differences in thermal sensitivity across depth (instantaneous acute heat stress, 5-10m *vs* 30-35m; Gould et al., 2021) or lower tolerance to acute heat stress in mesophotic colonies (ramping of 1°C/day; Frates et al., 2021). Our study is the first to present thermal performance of corals from lower mesophotic zone (45m at the deepest in previous studies). We unravelled distinct thermal performance of mesophotic colonies compared to mid-depth ones, with a broader thermal performance of mesophotic corals exposed to heat stress. Our results therefore suggest that high temperature variability (owing to internal waves activity) at mesophotic depths in French Polynesia likely contributes to the observed broader thermal performance of colonies from those depths.

Q_{10} results did not differ between depths, which does not support the higher thermotolerance of mesophotic colonies previously discussed based on the comparison of slopes between depths. This is counterintuitive as Q_{10} derives from the slope, but this is due to the different methods of calculation. Indeed, Q_{10} was first calculated on each individual subjected to the different temperatures and all Q_{10} were then averaged (mean $\pm$ sd), while slopes of the linear regressions were calculated based on all data together (and not individual colonies first). Q_{10} value therefore provides an indication of the variability of responses between depths, which was higher in mesophotic than in mid-depth colonies (Table 1). This higher variability in mesophotic colonies could be explained by the more fluctuating environmental conditions at these depths, and thus potentially a greater diversity in response strategies to these fluctuating conditions, compared to the mid-depth colonies that are exposed and have acclimated/adapted to more stable environmental conditions.

Comparing thermal performance of corals living at distinct depths has a real ecological interest if both shallow and deep zones are impacted by heat stress (e.g. marine heatwaves). MCEs are often viewed as areas of environmental stability, being spared by heat stress, which creates good conditions for the development and survival of corals compared to their shallow-water counterparts. However, MCEs may also be affected by heat stress and depending on the thermotolerance of corals living in these

areas, the consequences of heat stress affecting mesophotic reefs may be totally different. Although long-term temperature data at 85m were not available in French Polynesia, data were available from 3 to 50m and included the 2019 mass bleaching event around Mo'orea. These data confirmed ours in that temperature is colder and more variable in deeper areas of the reefs and they also revealed that the 2019 marine heatwave did not spare mesophotic depth, with a clear rise in temperature in both shallow and mesophotic areas (at least up to 50m; Fig. S1). This confirmed that mesophotic corals (at 50m) are impacted by heat stress and we could hypothesize that such heat stress was also present up to 85m. The suspected presence of heat stress at 85m, combined with the broader thermal performance of corals at 85m, support that mesophotic zone may serve as resistant oases (Guest et al., 2018) that are able to tolerate thermal anomaly without losing coral cover due to specific traits of the corals living there, as *P. speciosa*. We suggest that this is likely because mesophotic colonies, exposed to more variable seawater temperatures, developed broader thermal performance to withstand warming than their mid-depth congeners. This supports the assumption that mesophotic environments exposed to large thermal fluctuations, such as caused by internal waves, will be an important asset in the future from a management perspective, as they are most likely to be less susceptible to global warming than their shallower counterparts. We acknowledge that this observation of broader thermal performance of mesophotic corals was performed on a single species using acute heat stress. More endpoints at longer time scale and other depth-generalist species should be tested to confirm that pattern at a larger scale. In addition, even if bleaching was not observed *per se,* the increase in metabolic activity can be interpreted as an increase in sensitivity of the process (Silbiger et al., 2019), that could potentially lead to bleaching if exposure was extended over a longer period.

In contrast with previous parameters, the effect of temperature on photochemical efficiency (dark acclimated F_v/F_m) did not differ significantly between mid-depth and mesophotic colonies of *P. speciosa*. The relationship F_v/F_m according to temperature was described by a Gaussian function, with

493 a maximum (T_{opt}) at 26.2 and 27.8°C (at 25 and 85m, respectively) beyond which it started decreasing.
494 Moreover, 12 hours post-recovery, photochemical efficiency of the *Symbiodiniaceae* was not fully
495 recovered, at any depths. It is well known that, in darkness, oxygen concentration declines significantly
496 in coral tissues due to chlororespiration, leading to hypoxic conditions that results in a decline in F_v/F_m
497 of the symbionts during the night (Shashar et al., 1993; Jones et al., 2001). However, the addition of
498 exogenous oxygen to hypoxic coral tissues (held in darkness for several hours), as was continuously
499 provided during the ramping, was showed to be sufficient to increase F_v/F_m back to normal values
500 (Jones et al., 2001). So, we suggest that this decline in F_v/F_m around T_{opt} is unlikely to be an
501 experimental artefact. Rather, we suggest that it shows the rapid thermal acclimation capacity of the
502 symbionts. Indeed, T_{opt} (maximum F_v/F_m) was measured around 27°C at both depth, which corresponds
503 to the acclimation temperature. This suggests that an acclimation of 10 days at the common
504 temperature of 27°C was sufficient for the *Symbiodiniaceae* to optimize their photochemical efficiency.
505
506 *Pachyseris speciosa vs. Stichopathes sp.* from the same depth (85m)

507 At mesophotic depths, scleractinian corals co-exist with other cnidarians, including antipatharians. The
508 present study revealed distinct metabolic performances under thermal stress between *P. speciosa* and
509 *Stichopathes* sp. collected from the same site at 85m depth. Indeed, T_{opt} for dark respiration was
510 reached for *Stichopathes* sp. but not for *P. speciosa* and the higher sensitivity of *Stichopathes* sp. was
511 also supported by its high Q_{10} value, much out of the typical range of 2-3 for thermochemical enzymatic
512 reactions. Does that mean that *Stichopathes* sp. from Mo'orea is a (relatively) cold thermal specialist
513 and that its bathymetric range (from 60m and deeper) is constrained by temperature? Indeed, a
514 previous study of the same species showed that a 15d thermal exposure to 1°C above T_{opt} induced
515 deleterious effects (Godefroid et al., 2022). Reanalysing the data of Godefroid et al., (2022), using the
516 same Gaussian regression as in the present study, yielded a T_{opt} of 28.3°C and a T_{br} of 2.15°C. In the
517 present ramping experiment, T_{opt} was higher (29.6°C) and T_{br} was wider (4.26°C) than in Godefroid et
518 al. (2022), which is likely a consequence of seasonal acclimation, as the sampling was performed during

519 different sampling periods (February 2021 *vs*. October 2019 in Godefroid et al., 2022), which differed
520 in temperature (Figure S1). This mismatch could also be partly explained by the acute nature of the
521 stress performed, preventing acclimation to occur. Indeed, studies have previously showed that acute
522 ramping methodologies tend to overestimate T_{opt} in comparison with medium/long-term methods
523 (Schulte et al., 2011; Sinclair et al., 2016). Yet, differences in TPC metrics between the two
524 experimental approaches used (medium-term exposure in Godefroid et al., 2022 *vs* acute ramping in
525 the present study) were not significant (overlapping confidence intervals for each parameters, T_{br}, T_{opt}
526 and Pf_{max}). This indicates that the method used has limited influence on the results, supporting the use
527 of acute ramping methodologies for antipatharians (especially in a comparative approach).

528

529 **Conclusion**

530 No consensus currently exists as if Mesophotic Coral Ecosystems may or not provide resistant and/or
531 resilient coral oases to the increasing frequency of heat stress events. MCEs in Mo'orea were suggested
532 to play a role as short-term resistant oases from bleaching (Pérez-Rosales et al., 2021). Our study
533 contributed to this statement by providing the first metabolic evidence of a broader thermal
534 performance of the depth-generalist scleractinian *P. speciosa* at mesophotic depths compared to mid-
535 depth, which suggests the capacity of that species to adopt a thermal strategy depending on local
536 temperature regime. This supports that mesophotic environments exposed to large thermal
537 fluctuations are most likely to be more tolerant under global warming. Surprisingly, our work also shed
538 light on the constrained thermal performance of antipatharian compared to scleractinian, living in a
539 similar site at mesophotic depth (85m). This has important implication for predicting the future of
540 mesophotic reefs, as it unravelled that other biological processes than the *Symbiodiniaceae* symbiosis
541 may modulate the thermal performance of benthic organisms in that particular zone of the reefs.
542 Regarding the lack of plasticity of antipatharian compared to scleractinian in response to heat stress,

it is unlikely to observe a shift of dominance from scleractinian to antipatharian in future mesophotic reefs.

CRediT author statement

Godefroid Mathilde: Conceptualization, Methodology, Formal Analysis, Investigation, Writing: Original Draft, Review and Editing; **Philippe Dubois:** Conceptualization, Methodology, Writing: Review and Editing; **Under The Pole Consortium:** Resources; **Laetitia Hédouin:** Conceptualization, Methodology, Writing: Review and Editing.

Acknowledgements

M. Godefroid is holder of a Belgian FRIA grant (FRS-FNRS, number 1.E.066.19F). Ph. Dubois is a Research Director of the National Fund for Scientific Research (FRS-FNRS; Belgium). L. Hédouin is a CNRS Research Fellow (France). This work was supported by the FNRS projet COBICO (T0084.18), the ANR DEEPHOPE (ANRAAPG 2017 grant no. 168722), the Délégation à la Recherche DEEPCORAL, the CNRS DEEPREEF, the Agence Française pour la Biodiversité POLYAFB and the IFRECOR. We sincerely thank G. Iwankow for his help in the collection of the colonies, A. Mercière and Y. Lacube for their advices with the setup of the aquarium system. Service d'Observation CORAIL (SO Corail) from CRIOBE kindly provided the temperature data (Figure S1). We thank the different reviewers for their significant contribution in improving the final version of the manuscript. Under The Pole Consortium: G. Bardout, A. Ferucci, F. Gazzola, G. Lagarrigue, J. Leblond, E. Marivint, N. Mollon, N. Paulme, E. Périé-Bardout, S. Pujolle, G. Siu. The authors have no conflicts of interest to declare.

References

566 Aichelman, H. E., Zimmerman, R. C., & Barshis, D. J. (2019). Adaptive signatures in thermal
567 performance of the temperate coral *Astrangia poculata*. *The Journal of Experimental Biology*,
568 *222*(5), jeb189225. https://doi.org/10.1242/jeb.189225
569 Angilletta, M. J. (2009). *Thermal adaptation: A theoretical and empirical synthesis*. Oxford University
570 Press.
571 Barshis, D. J., Birkeland, C., Toonen, R. J., Gates, R. D., & Stillman, J. H. (2018). High-frequency
572 temperature variability mirrors fixed differences in thermal limits of the massive coral *Porites*
573 *lobata* (Dana, 1846). *Journal of Experimental Biology*. https://doi.org/10.1242/jeb.188581
574 Ben-Zvi, O., Ofer, E., Eyal, G., & Loya, Y. (2021). Experimental evidence of temperature-induced
575 bleaching in two fluorescence morphs of a Red Sea mesophotic coral. *Coral Reefs*, *40*(1),
576 187–199. https://doi.org/10.1007/s00338-020-02027-0
577 Blois, J. L., Williams, J. W., Fitzpatrick, M. C., Jackson, S. T., & Ferrier, S. (2013). Space can substitute
578 for time in predicting climate-change effects on biodiversity. *Proceedings of the National*
579 *Academy of Sciences*, *110*(23), 9374–9379. https://doi.org/10.1073/pnas.1220228110
580 Bo, M., Baker, A., Gaino, E., Wirshing, H., Scoccia, F., & Bavestrello, G. (2011). First description of
581 algal mutualistic endosymbiosis in a black coral (Anthozoa: Antipatharia). *Marine Ecology*
582 *Progress Series*, *435*, 1–11. https://doi.org/10.3354/meps09228
583 Bo, M., Bavestrello, G., Barucca, M., Makapedua, D. M., Poliseno, A., Forconi, M., Olmo, E., & Canapa,
584 A. (2012). Morphological and molecular characterization of the problematic whip black coral
585 genus Stichopathes (Hexacorallia: Antipatharia) from Indonesia (North Sulawesi, Celebes
586 Sea): Taxonomy of the genus *Stichopathes* from Indonesia. *Zoological Journal of the Linnean*
587 *Society*, no-no. https://doi.org/10.1111/j.1096-3642.2012.00834.x
588 Bo, M., Bavestrello, G., Di Muzio, G., Canese, S., & Betti, F. (2019). First record of a symbiotic
589 relationship between a polyclad and a black coral with description of Anthoplana
590 antipathellae gen. Et sp. Nov. (Acotylea, Notoplanidae). *Marine Biodiversity*.
591 https://doi.org/10.1007/s12526-019-00982-8

592 Bo, M., Rouse, G. W., Martin, D., & Bavestrello, G. (2014). A myzostomid endoparasitic in black
593 corals. *Coral Reefs*, *33*(1), 273–273. https://doi.org/10.1007/s00338-013-1095-0
594 Bongaerts, P., Ridgway, T., Sampayo, E. M., & Hoegh-Guldberg, O. (2010). Assessing the 'deep reef
595 refugia' hypothesis: Focus on Caribbean reefs. *Coral Reefs*, *29*(2), 309–327.
596 https://doi.org/10.1007/s00338-009-0581-x
597 Castillo, K. D., & Helmuth, B. S. T. (2005). Influence of thermal history on the response of
598 Montastraea annularis to short-term temperature exposure. *Marine Biology*, *148*(2), 261–
599 270. https://doi.org/10.1007/s00227-005-0046-x
600 Chown, S. L., Jumbam, K. R., Sørensen, J. G., & Terblanche, J. S. (2009). Phenotypic variance, plasticity
601 and heritability estimates of critical thermal limits depend on methodological context.
602 *Functional Ecology*, *23*(1), 133–140. https://doi.org/10.1111/j.1365-2435.2008.01481.x
603 De Clippele, L. H., Huvenne, V. A. I., Molodtsova, T. N., & Roberts, J. M. (2019). The Diversity and
604 Ecological Role of Non-scleractinian Corals (Antipatharia and Alcyonacea) on Scleractinian
605 Cold-Water Coral Mounds. *Frontiers in Marine Science*, *6*.
606 https://doi.org/10.3389/fmars.2019.00184
607 Deutsch, C. A., Tewksbury, J. J., Huey, R. B., Sheldon, K. S., Ghalambor, C. K., Haak, D. C., & Martin, P.
608 R. (2008). Impacts of climate warming on terrestrial ectotherms across latitude. *Proceedings*
609 *of the National Academy of Sciences*, *105*(18), 6668–6672.
610 https://doi.org/10.1073/pnas.0709472105
611 Ferrier-Pagès, C., Bednarz, V., Grover, R., Benayahu, Y., Maguer, J., Rottier, C., Wiedenmann, J., &
612 Fine, M. (2022). Symbiotic stony and soft corals: Is their host-algae relationship really
613 mutualistic at lower mesophotic reefs? *Limnology and Oceanography*, *67*(1), 261–271.
614 https://doi.org/10.1002/lno.11990
615 Fitt, W., Brown, B., Warner, M., & Dunne, R. (2001). Coral bleaching: Interpretation of thermal
616 tolerance limits and thermal thresholds in tropical corals. *Coral Reefs*, *20*(1), 51–65.
617 https://doi.org/10.1007/s003380100146

618 Fitt, W. K., Dunne, R. P., Gibb, S. W., Cummings, D. G., Ambarsari, I., Brown, B. E., & Warner, M. E.
619 (1999). Diurnal changes in photochemical efficiency and xanthophyll concentrations in
620 shallow water reef corals: Evidence for photoinhibition and photoprotection. *Coral Reefs*,
621 *18*(2), 99–105. https://doi.org/10.1007/s003380050163
622 Fitt, W. K., McFarland, F. K., Warner, M. E., & Chilcoat, G. C. (2000). Seasonal patterns of tissue
623 biomass and densities of symbiotic dinoflagellates in reef corals and relation to coral
624 bleaching. *Limnology and oceanography*, *45*(3), 677-685.
625 Frade, P. R., Bongaerts, P., Englebert, N., Rogers, A., Gonzalez-Rivero, M., & Hoegh-Guldberg, O.
626 (2018). Deep reefs of the Great Barrier Reef offer limited thermal refuge during mass coral
627 bleaching. *Nature Communications*, *9*(1). https://doi.org/10.1038/s41467-018-05741-0
628 Frates, E., Hughes, A., & Randall, A. (n.d.). *Orbicella faveolata: Shallow Versus Mesophotic Coral*
629 *Responses to Temperature Change*. 15.
630 Gaston, K. J., Chown, S. L., Calosi, P., Bernardo, J., Bilton, D. T., Clarke, A., Clusella-Trullas, S.,
631 Ghalambor, C. K., Konarzewski, M., Peck, L. S., Porter, W. P., Pörtner, H. O., Rezende, E. L.,
632 Schulte, P. M., Spicer, J. I., Stillman, J. H., Terblanche, J. S., & van Kleunen, M. (2009).
633 Macrophysiology: A Conceptual Reunification. *The American Naturalist*, *174*(5), 595–612.
634 https://doi.org/10.1086/605982
635 Ghalambor, C. K. (2006). Are mountain passes higher in the tropics? Janzen's hypothesis revisited.
636 *Integrative and Comparative Biology*, *46*(1), 5–17. https://doi.org/10.1093/icb/icj003
637 Glynn, P. W. (1996). Coral reef bleaching: Facts, hypotheses and implications. *Global Change Biology*,
638 *2*(6), 495–509. https://doi.org/10.1111/j.1365-2486.1996.tb00063.x
639 Godefroid, M., Hédouin, L., Mercière, A., & Dubois, P. (2022). Thermal stress responses of the
640 antipatharian Stichopathes sp. From the mesophotic reef of Mo'orea, French Polynesia.
641 *Science of The Total Environment*, *820*, 153094.
642 https://doi.org/10.1016/j.scitotenv.2022.153094

643 Gould, K., Bruno, J. F., Ju, R., & Goodbody-Gringley, G. (2021). Upper-mesophotic and shallow reef
644 corals exhibit similar thermal tolerance, sensitivity and optima. *Coral Reefs*, *40*(3), 907–920.
645 https://doi.org/10.1007/s00338-021-02095-w
646 Gress, E., Eeckhaut, I., Godefroid, M., Dubois, P., Richir, J., & Terrana, L. (2021). *Investigating*
647 *densities of Symbiodiniaceae in two species of Antipatharians (black corals) from Madagascar*
648 [Preprint]. Molecular Biology. https://doi.org/10.1101/2021.01.22.427691
649 Guest, J. R., Baird, A. H., Maynard, J. A., Muttaqin, E., Edwards, A. J., Campbell, S. J., Yewdall, K.,
650 Affendi, Y. A., & Chou, L. M. (2012). Contrasting Patterns of Coral Bleaching Susceptibility in
651 2010 Suggest an Adaptive Response to Thermal Stress. *PLoS ONE*, *7*(3), e33353.
652 https://doi.org/10.1371/journal.pone.0033353
653 Guest, J. R., Edmunds, P. J., Gates, R. D., Kuffner, I. B., Andersson, A. J., Barnes, B. B., Chollett, I.,
654 Courtney, T. A., Elahi, R., Gross, K., Lenz, E. A., Mitarai, S., Mumby, P. J., Nelson, H. R., Parker,
655 B. A., Putnam, H. M., Rogers, C. S., & Toth, L. T. (2018). A framework for identifying and
656 characterising coral reef "oases" against a backdrop of degradation. *Journal of Applied*
657 *Ecology*, *55*(6), 2865–2875. https://doi.org/10.1111/1365-2664.13179
658 Gunderson, A. R., & Stillman, J. H. (2015). Plasticity in thermal tolerance has limited potential to
659 buffer ectotherms from global warming. *Proceedings of the Royal Society B: Biological*
660 *Sciences*, *282*(1808), 20150401. https://doi.org/10.1098/rspb.2015.0401
661 Hinderstein, L. M., Marr, J. C. A., Martinez, F. A., Dowgiallo, M. J., Puglise, K. A., Pyle, R. L., Zawada, D.
662 G., & Appeldoorn, R. (2010). Theme section on "Mesophotic Coral Ecosystems:
663 Characterization, Ecology, and Management". *Coral Reefs*, *29*(2), 247–251.
664 https://doi.org/10.1007/s00338-010-0614-5
665 Huey, R. B., Deutsch, C. A., Tewksbury, J. J., Vitt, L. J., Hertz, P. E., Álvarez Pérez, H. J., & Garland, T.
666 (2009). Why tropical forest lizards are vulnerable to climate warming. *Proceedings of the*
667 *Royal Society B: Biological Sciences*, *276*(1664), 1939–1948.
668 https://doi.org/10.1098/rspb.2008.1957

669 Huey, R., & Stevenson, R. (1979). Integrating thermal physiology and ecology of ectotherms: A
670 discussion of approaches. *Am Zool*, *19*, 357–366.
671 Kahng, S. E., Akkaynak, D., Shlesinger, T., Hochberg, E. J., Wiedenmann, J., Tamir, R., & Tchernov, D.
672 (2019). Light, Temperature, Photosynthesis, Heterotrophy, and the Lower Depth Limits of
673 Mesophotic Coral Ecosystems. In Y. Loya, K. A. Puglise, & T. C. L. Bridge (Eds.), *Mesophotic*
674 *Coral Ecosystems* (Vol. 12, pp. 801–828). Springer International Publishing.
675 https://doi.org/10.1007/978-3-319-92735-0_42
676 Kenkel, C. D., Goodbody-Gringley, G., Caillaud, D., Davies, S. W., Bartels, E., & Matz, M. V. (2013).
677 Evidence for a host role in thermotolerance divergence between populations of the mustard
678 hill coral (*Porites astreoides*) from different reef environments. *Molecular Ecology*, *22*(16),
679 4335–4348. https://doi.org/10.1111/mec.12391
680 Kenkel, C. D., Setta, S. P., & Matz, M. V. (2015). Heritable differences in fitness-related traits among
681 populations of the mustard hill coral, Porites astreoides. *Heredity*, *115*(6), 509–516.
682 https://doi.org/10.1038/hdy.2015.52
683 Kingsolver, J. G., Gomulkiewicz, R., & Carter, P. A. (2001). Variation, selection and evolution of
684 function-valued traits. In A. P. Hendry & M. T. Kinnison (Eds.), *Microevolution Rate, Pattern,*
685 *Process* (Vol. 8, pp. 87–104). Springer Netherlands. https://doi.org/10.1007/978-94-010-
686 0585-2_7
687 Leichter, J. J., Helmuth, B., & Fischer, A. M. (2006). Variation beneath the surface: Quantifying
688 complex thermal environments on coral reefs in the Caribbean, Bahamas and Florida. *Journal*
689 *of Marine Research*, *64*(4), 563–588. https://doi.org/10.1357/002224006778715711
690 Leichter, J. J., Stokes, M. D., Hench, J. L., Witting, J., & Washburn, L. (2012). The island-scale internal
691 wave climate of Moorea, French Polynesia: internal waves on Mo'orea. *Journal of*
692 *Geophysical Research: Oceans*, *117*(C6), n/a-n/a. https://doi.org/10.1029/2012JC007949
693 Leichter, J. J., Stokes, M. D., Vilchis, L. I., & Fiechter, J. (2014). Regional synchrony of temperature
694 variation and internal wave forcing along the Florida Keys reef tract: Regional synchrony of

internal waves. *Journal of Geophysical Research: Oceans*, *119*(1), 548–558. https://doi.org/10.1002/2013JC009371

Leletkin, V. A., Titlyanov, E. A., & Dubinsky, Z. (1996). Photosynthesis and respiration of the zooxanthellae in hermatypic corals habitated on different depths of the Gulf of Filat. *Photosynthetica*, *32*(4), 481-490.

Lesser, M. P., Slattery, M., & Leichter, J. J. (2009). Ecology of mesophotic coral reefs. *Journal of Experimental Marine Biology and Ecology*, *375*(1–2), 1–8. https://doi.org/10.1016/j.jembe.2009.05.009

Loya, Y., Puglise, K. A., & Bridge, T. C. L. (Eds.). (2019). *Mesophotic Coral Ecosystems* (Vol. 12). Springer International Publishing. https://doi.org/10.1007/978-3-319-92735-0

Mass, T., Kline, D. I., Roopin, M., Veal, C. J., Cohen, S., Iluz, D., & Levy, O. (2010). The spectral quality of light is a key driver of photosynthesis and photoadaptation in *Stylophora pistillata* colonies from different depths in the Red Sea. *Journal of Experimental Biology*, *213*(23), 4084-4091.

Millero, F. J., & Huang, F. (2009). The density of seawater as a function of salinity (5 to 70 g kg^{-1}) and temperature (273.15 to 363.15 K). *Ocean Science*, *5*(2), 91–100. https://doi.org/10.5194/os-5-91-2009

Millero, F. J., & Poisson, A. (1981). International one-atmosphere equation of state of seawater. *Deep Sea Research Part A. Oceanographic Research Papers*, *28*(6), 625–629. https://doi.org/10.1016/0198-0149(81)90122-9

Mitchell, K. A., & Hoffmann, A. A. (2010). Thermal ramping rate influences evolutionary potential and species differences for upper thermal limits in *Drosophila*: *Limited h ^{2} and reduced thermal limits in* Drosophila. *Functional Ecology*, *24*(3), 694–700. https://doi.org/10.1111/j.1365-2435.2009.01666.x

718 Mora, C., & Maya, M. F. (2006). Effect of the rate of temperature increase of the dynamic method on
719 the heat tolerance of fishes. *Journal of Thermal Biology*, *31*(4), 337–341.
720 https://doi.org/10.1016/j.jtherbio.2006.01.005
721 Oliver, T. A., & Palumbi, S. R. (2011). Do fluctuating temperature environments elevate coral thermal
722 tolerance? *Coral Reefs*, *30*(2), 429–440. https://doi.org/10.1007/s00338-011-0721-y
723 Opresko, D. M., Tracey, D. M., Mackay, E., New Zealand, & Ministry for Primary Industries. (2014).
724 *Antipatharia (Black Corals) for the New Zealand region: A field guide of commonly sampled*
725 *New Zealand black corals including illustrations highlighting technical terms and black coral*
726 *morphology*.
727 Padilla-Gamiño, J. L., Roth, M. S., Rodrigues, L. J., Bradley, C. J., Bidigare, R. R., Gates, R. D., ... &
728 Spalding, H. L. (2019). Ecophysiology of mesophotic reef-building corals in Hawai 'i is
729 influenced by symbiont–host associations, photoacclimatization, trophic plasticity, and
730 adaptation. *Limnology and Oceanography*, *64*(5), 1980-1995.
731 Page, C. E., Leggat, W., Heron, S. F., Choukroun, S. M., Lloyd, J., & Ainsworth, T. D. (2019). Seeking
732 Resistance in Coral Reef Ecosystems: The Interplay of Biophysical Factors and Bleaching
733 Resistance under a Changing Climate: The Interplay of a Reef's Biophysical Factors Can
734 Mitigate the Coral Bleaching Response. *BioEssays*, *41*(7), 1800226.
735 https://doi.org/10.1002/bies.201800226
736 Pérez-Rosales, G., Rouzé, H., Torda, G., Bongaerts, P., Pichon, M., Under The Pole Consortium,
737 Parravicini, V., & Hédouin, L. (2021). Mesophotic coral communities escape thermal coral
738 bleaching in French Polynesia. *Royal Society Open Science*, *8*(11).
739 https://doi.org/10.1098/rsos.210139
740 Pichon, M. (2019). French Polynesia. In Y. Loya, K. A. Puglise, & T. C. L. Bridge (Eds.), *Mesophotic Coral*
741 *Ecosystems* (Vol. 12, pp. 425–443). Springer International Publishing.
742 https://doi.org/10.1007/978-3-319-92735-0_24

743 Pickett, S. T. A. (1989). Space-for-Time Substitution as an Alternative to Long-Term Studies. In G. E.
744 Likens (Ed.), *Long-Term Studies in Ecology* (pp. 110–135). Springer New York.
745 https://doi.org/10.1007/978-1-4615-7358-6_5
746 Piniak, G. A., & Storlazzi, C. D. (2008). Diurnal variability in turbidity and coral fluorescence on a
747 fringing reef flat: Southern Molokai, Hawaii. *Estuarine, Coastal and Shelf Science*, *77*(1), 56–
748 64. https://doi.org/10.1016/j.ecss.2007.08.023
749 Rezende, E. L., Tejedo, M., & Santos, M. (2011). Estimating the adaptive potential of critical thermal
750 limits: Methodological problems and evolutionary implications. *Functional Ecology*, *25*(1),
751 111–121. https://doi.org/10.1111/j.1365-2435.2010.01778.x
752 Rocha, L. A., Pinheiro, H. T., Shepherd, B., Papastamatiou, Y. P., Luiz, O. J., Pyle, R. L., & Bongaerts, P.
753 (2018). Mesophotic coral ecosystems are threatened and ecologically distinct from shallow
754 water reefs. *Science*, *361*(6399), 281–284. https://doi.org/10.1126/science.aaq1614
755 Rodolfo-Metalpa, R., Hoogenboom, M. O., Rottier, C., Ramos-Esplá, A., Baker, A. C., Fine, M., &
756 Ferrier-Pagès, C. (2014). Thermally tolerant corals have limited capacity to acclimatize to
757 future warming. *Global Change Biology*, *20*(10), 3036–3049.
758 https://doi.org/10.1111/gcb.12571
759 Rossi, S., Bramanti, L., Gori, A., & Orejas, C. (Eds.). (2017). *Marine Animal Forests: The Ecology of*
760 *Benthic Biodiversity Hotspots*. Springer International Publishing.
761 https://doi.org/10.1007/978-3-319-17001-5
762 Safaie, A., Silbiger, N. J., McClanahan, T. R., Pawlak, G., Barshis, D. J., Hench, J. L., Rogers, J. S.,
763 Williams, G. J., & Davis, K. A. (2018). High frequency temperature variability reduces the risk
764 of coral bleaching. *Nature Communications*, *9*(1). https://doi.org/10.1038/s41467-018-
765 04074-2
766 Schulte, P. M. (2015). The effects of temperature on aerobic metabolism: Towards a mechanistic
767 understanding of the responses of ectotherms to a changing environment. *Journal of*
768 *Experimental Biology*, *218*(12), 1856–1866. https://doi.org/10.1242/jeb.118851

769 Schulte, P. M., Healy, T. M., & Fangue, N. A. (2011). Thermal Performance Curves, Phenotypic
770 Plasticity, and the Time Scales of Temperature Exposure. *Integrative and Comparative*
771 *Biology*, *51*(5), 691–702. https://doi.org/10.1093/icb/icr097
772 Seebacher, F., White, C. R., & Franklin, C. E. (2015). Physiological plasticity increases resilience of
773 ectothermic animals to climate change. *Nature Climate Change*, *5*(1), 61–66.
774 https://doi.org/10.1038/nclimate2457
775 Shah, A. A., Funk, W. C., & Ghalambor, C. K. (2017). Thermal Acclimation Ability Varies in Temperate
776 and Tropical Aquatic Insects from Different Elevations. *Integrative and Comparative Biology*,
777 *57*(5), 977–987. https://doi.org/10.1093/icb/icx101
778 Shah, A. A., Gill, B. A., Encalada, A. C., Flecker, A. S., Funk, W. C., Guayasamin, J. M., Kondratieff, B. C.,
779 Poff, N. L., Thomas, S. A., Zamudio, K. R., & Ghalambor, C. K. (2017). Climate variability
780 predicts thermal limits of aquatic insects across elevation and latitude. *Functional Ecology*,
781 *31*(11), 2118–2127. https://doi.org/10.1111/1365-2435.12906
782 Sheppard, C. (2009). Large temperature plunges recorded by data loggers at different depths on an
783 Indian Ocean atoll: Comparison with satellite data and relevance to coral refuges. *Coral*
784 *Reefs*, *28*(2), 399–403. https://doi.org/10.1007/s00338-009-0476-x
785 Silbiger, N. J., Goodbody-Gringley, G., Bruno, J. F., & Putnam, H. M. (2019). Comparative thermal
786 performance of the reef-building coral *Orbicella franksi* at its latitudinal range limits. *Marine*
787 *Biology*, *166*(10). https://doi.org/10.1007/s00227-019-3573-6
788 Sinclair, B. J., Marshall, K. E., Sewell, M. A., Levesque, D. L., Willett, C. S., Slotsbo, S., Dong, Y., Harley,
789 C. D. G., Marshall, D. J., Helmuth, B. S., & Huey, R. B. (2016). Can we predict ectotherm
790 responses to climate change using thermal performance curves and body temperatures?
791 *Ecology Letters*, *19*(11), 1372–1385. https://doi.org/10.1111/ele.12686
792 Smith, T. B., Gyory, J., Brandt, M. E., Miller, W. J., Jossart, J., & Nemeth, R. S. (2016). Caribbean
793 mesophotic coral ecosystems are unlikely climate change refugia. *Global Change Biology*,
794 *22*(8), 2756–2765. https://doi.org/10.1111/gcb.13175

795 Smith, E. G., D'angelo, C., Sharon, Y., Tchernov, D., & Wiedenmann, J. (2017). Acclimatization of
796 symbiotic corals to mesophotic light environments through wavelength transformation by
797 fluorescent protein pigments. *Proceedings of the Royal Society B: Biological*
798 *Sciences*, *284*(1858), 20170320.

799 Sunday, J. M., Bates, A. E., & Dulvy, N. K. (2012). Thermal tolerance and the global redistribution of
800 animals. *Nature Climate Change*, *2*(9), 686–690. https://doi.org/10.1038/nclimate1539
801 Terblanche, J. S., Deere, J. A., Clusella-Trullas, S., Janion, C., & Chown, S. L. (2007). Critical thermal
802 limits depend on methodological context. *Proceedings of the Royal Society B: Biological*
803 *Sciences*, *274*(1628), 2935–2943. https://doi.org/10.1098/rspb.2007.0985
804 Terrana, L., Lepoint, G., & Eeckhaut, I. (2019). Assessing trophic relationships between shallow-water
805 black corals (Antipatharia) and their symbionts using stable isotopes. *Belgian Journal of*
806 *Zoology*, *149*(1). https://doi.org/10.26496/bjz.2019.33
807 Tewksbury, J. J., Huey, R. B., & Deutsch, C. A. (2008). Putting the Heat on Tropical Animals. *Science*,
808 *320*(5881), 1296–1297. https://doi.org/10.1126/science.1159328
809 Thornhill, D. J., Kemp, D. W., Bruns, B. U., Fitt, W. K., & Schmidt, G. W. (2008). Correspondence
810 between cold tolerance and temperate biogeography in a Western Atlantic Symbiodinium
811 (Dinophyta) lineage. *Journal of Phycology*, *44*(5), 1126–1135. https://doi.org/10.1111/j.1529-
812 8817.2008.00567.x
813 Venegas, R. M., Oliver, T., Liu, G., Heron, S. F., Clark, S. J., Pomeroy, N., Young, C., Eakin, C. M., &
814 Brainard, R. E. (2019). The Rarity of Depth Refugia from Coral Bleaching Heat Stress in the
815 Western and Central Pacific Islands. *Scientific Reports*, *9*(1). https://doi.org/10.1038/s41598-
816 019-56232-1
817 Wagner, D., Luck, D. G., & Toonen, R. J. (2012). The Biology and Ecology of Black Corals (Cnidaria:
818 Anthozoa: Hexacorallia: Antipatharia). In *Advances in Marine Biology* (Vol. 63, pp. 67–132).
819 Elsevier. https://doi.org/10.1016/B978-0-12-394282-1.00002-8

820 Wagner, D., Pochon, X., Irwin, L., Toonen, R. J., & Gates, R. D. (2011). Azooxanthellate? Most
821 Hawaiian black corals contain Symbiodinium. *Proceedings of the Royal Society B: Biological*
822 *Sciences*, *278*(1710), 1323–1328. https://doi.org/10.1098/rspb.2010.1681
823 Wall, M., Putchim, L., Schmidt, G. M., Jantzen, C., Khokiattiwong, S., & Richter, C. (2015). Large-
824 amplitude internal waves benefit corals during thermal stress. *Proceedings of the Royal*
825 *Society B: Biological Sciences*, *282*(1799), 20140650. https://doi.org/10.1098/rspb.2014.0650
826 Wolanski, E., Colin, P., Naithani, J., Deleersnijder, E., & Golbuu, Y. (2004). Large amplitude, leaky,
827 island-generated, internal waves around Palau, Micronesia. *Estuarine, Coastal and Shelf*
828 *Science*, *60*(4), 705–716. https://doi.org/10.1016/j.ecss.2004.03.009
829 Wyatt, A. S. J., Leichter, J. J., Toth, L. T., Miyajima, T., Aronson, R. B., & Nagata, T. (2020). Heat
830 accumulation on coral reefs mitigated by internal waves. *Nature Geoscience*, *13*(1), 28–34.
831 https://doi.org/10.1038/s41561-019-0486-4
832